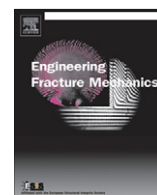




Contents lists available at ScienceDirect

Engineering Fracture Mechanics

journal homepage: www.elsevier.com/locate/engfracmech

Optimum location of a three strain gauge rosette for measuring mixed mode stress intensity factors

A. Dorogoy*, D. Rittel

Faculty of Mechanical Engineering, Technion – Israel Institute of Technology, Technion City, 32000 Haifa, Israel

ARTICLE INFO

Article history:

Received 20 July 2007

Received in revised form 29 February 2008

Accepted 26 March 2008

Available online xxxx

Keywords:

Rosette

Strain gauge

Stress intensity factors

Mixed mode

Error

ABSTRACT

This paper analyzes the errors inherent to the determination of mixed mode stress intensity factors from data obtained by using a three strain gauge rosette. The analysis shows that the errors are mainly due the third characteristic value ($3/2$) and its corresponding coefficients. It is also shown that the errors do not depend on the orientation angle of the rosette, the angle between the strain gauges and the material properties. The error mainly depends on its location (radius, angle), being linear in the radius. For pure mode I, an angle of 90° will completely eliminate the error due to the angle, while for pure mode II, a 0° angle will minimize it. The normalized variation of the errors with the angle at any radius is shown for different ratios of the corresponding coefficients of the third characteristic value. The analytical results are applied to a numerical example of an edge crack subjected to mixed mode loading. From the numerical example, it is recommended to use two strain gauge rosettes at the same angle, and linearly extrapolate their results, if errors less than 15% for a mixed mode field are desired.

© 2008 Elsevier Ltd. All rights reserved.

1. Introduction

Strain gauges are the most widespread device to date in experimental stress analysis. This is due their relatively low cost, non-invasiveness and ease of use in most environments [1]. The fracture mechanics of both stationary and propagating cracks in homogenous materials or interfaces has been extensively investigated using strain gauges. The accuracy of determination of the stress intensity factors depends on the gauge location and orientation relative to the crack tip. A few examples of the applications of strain gauges to fracture problems follows.

Dally and Sanford [2] developed expressions for the strains in a valid region adjacent to the crack tip, and indicated procedures for locating and orienting the gauges to accurately determine K_I from one or more strain gauge readings. In [3], a row of strain gauges was placed at a constant distance above the crack line, and each gauge is oriented such as to eliminate the T stress for measuring the K_I value of a straight crack propagating in an isotropic plate. Shukla et al. [4] used strain gauges to determine mode I stress intensity factor in orthotropic composite. Only one strain gauge was used in to determine the K_I in [5] and [6], as well as K_{II} in [7]. K_I was determined in [8] using two strain gauges. These authors have achieved errors less than 5% with an appropriate location of the strain gauges. Multiple strain gauges [10] were used in [9] to determine the mixed mode parameters of a sharp notch. A strain gauge rosette comprising two gauges and a single strain gauge were used to determine the T and K_I in [10]. Ricci et al. [11] developed a technique for determining the complex stress intensity factor of a bimaterial crack. They used two strain gauges at two different locations. The orientations were kept to a fixed θ direction, and the effect of the orientation angle on the accuracy was not investigated. Marur and Tippur [12] also developed a simple

* Corresponding author.

E-mail address: dorogoy@technion.ac.il (A. Dorogoy).

Nomenclature

a	crack length
a_0, a_1	functions of the coordinates and material properties corresponding to the asymptotic solution coefficients A_0, A_1 , respectively
b	width of a plate
b_0, b_1	functions of the coordinates and material properties corresponding to the asymptotic solution coefficients B_0, B_1 , respectively
c_1	function of the coordinates and material properties corresponding to the asymptotic solution coefficients C_1
d_i	a name vector containing the names $[a_0, b_0, a_1, b_1, c_1]^T$
f_i	a vector of functions containing the functions $[a_0, b_0, a_1, b_1, c_1]^T$
n, k	integers
r	radial coordinate
A_0, A_1	the first two coefficients corresponding to mode I asymptotic solution of a crack with the eigenvalues λ_n
B_0, B_1	the first two coefficients corresponding to mode II asymptotic solution of a crack with the eigenvalues λ_n
B_0, B_1	the first coefficients corresponding to mode I asymptotic solution of a crack with the eigenvalues μ_k
D_1	the first coefficients corresponding to mode II asymptotic solution of a crack with the eigenvalues μ_k
E	Young's modulus
E_r	a vector containing expressions for the errors in calculating $[A_0, B_0, C_1]^T$
$r(\theta)$	normalized vector of errors $E_r/(r\sqrt{A_1^2 + B_1^2})$
K_I, K_{II}	stress intensity factors of mode I and mode II, respectively
K_0	stress intensity factor $K_0 = \sigma_0\sqrt{\pi a}$
M	a 3×3 matrix relating linearly the three measured strains to the coefficients $[A_0, B_0, C_1]^T$
R	a vector containing the main truncation errors $[R_1, R_2, R_3]^T$ in calculating the coefficients $[A_0, B_0, C_1]^T$ from the three measured strains of the gauge
R_1, R_2, R_3	the truncation errors of the three gauges oriented in directions $\alpha_1, \alpha_2, \alpha_3$, respectively
T	stress parallel to the crack face due to mode I loading and $\mu_1 = 1$
α	orientation angle of a strain gauge
α_0	orientation angle which eliminate the T stress
$\alpha_1, \alpha_2, \alpha_3$	orientations angles of the three strain gauges of the rosette
β	angle between the gauges of the rosette
λ_n^*	all eigenvalues of the crack solution: $\lambda_n^* = \frac{n}{2}, n = 1 \dots \infty$
λ_n	part of λ_n^* which include the eigenvalues: $\lambda_n = n + \frac{1}{2}, n = 0 \dots \infty$
μ_k	part of λ_n^* which include the eigenvalues: $\mu_k = k, k = 1 \dots \infty$
ε	a vector containing $[\varepsilon_1, \varepsilon_2, \varepsilon_3]^T$
$\varepsilon_1, \varepsilon_2, \varepsilon_3$	the measured strains of a rosette in directions $\alpha_1, \alpha_2, \alpha_3$ correspondingly
$\varepsilon_{rr}, \varepsilon_{\theta\theta}, \varepsilon_{r\theta}$	strain in a polar coordinate system (r, θ)
$\varepsilon_{\alpha\alpha}$	strain in direction α
K_{II}	Poisson's ratio
θ	polar coordinate
σ_0	stress applied in the far field
ψ	angle between the coefficients A_1 and B_1 : $\tan \psi = \frac{B_1}{A_1}$

technique for determining the complex stress intensity factor of a bimaterial crack. They used a biaxial rosette to measure the radial and hoop strains. The use of the biaxial rosette instead of two separate gauges as in [11] was meant to improve accuracy in dynamic loading where separate locations might experience different stress conditions. This technique was used in [13] to determine the interfacial fracture parameters of bimaterial and functionally graded materials under impact loading conditions.

The application of a three strain gauge rosette in a mixed mode static or dynamic loading where T stresses might be present was not addressed.

The above mentioned works make essentially use of single strain gauges or two-gauge rosettes. Yet, the three strain gauge rosette has the advantage of providing the first three coefficients of the asymptotic expansion at one point, with a clear advantage for dynamic loading situations, while preserving space. This paper analyses the errors involved in this application and discusses an optimum location and orientation of such a rosette.

The paper is organized as follows: first the formulation of the strain $\varepsilon_{\alpha\alpha}$ at a point (r, θ) close to the crack tip in α direction is given explicitly using the first five terms of the asymptotic expansion. Then the formulation is applied to determine analytically the optimum location and orientation for a single strain gauge and a three gauge rosette. The analysis is followed by a numerical example of an inclined edge crack in a finite plate subjected to tension. The main results are then discussed followed by a concluding section.

2. Calculation of stress intensity factors from experimental results: linear elastic case

The stress intensity factors (SIFs) are calculated by fitting the measured strains to the asymptotic solution of the crack tip fields in a homogeneous, linear elastic material, as shown by Irwin [14] and Williams [15] (see Appendix A). A strain gauge is located at a distance (r, θ) from the crack tip, and oriented at an angle α as shown in Fig. 1.

The eigenvalues $\lambda_n^* = \frac{n}{2}$, $n \geq 1$ of the asymptotic solution are divided into two sets of eigenvalues $\mu_k = k$, $k = 1 \dots \infty$ and $\lambda_n = n + \frac{1}{2}$, $n = 0 \dots \infty$. The coefficients A_i and B_i are coefficients of the asymptotic expansion corresponding to λ_n . The coefficients C_i and D_i are coefficients of the asymptotic expansion due to μ_k . A_i and C_i correspond to mode I loading while B_i and D_i correspond to mode II loading. The complete solution is a superposition of the eigenfunctions of all the different eigenvalues. The singular terms are due to $\lambda_0 = \frac{1}{2}$ when $n = 0$ and the stress intensity factors are related to the first coefficients by: $K_I = \frac{\sqrt{2\pi}}{2} A_0$, $K_{II} = \frac{\sqrt{2\pi}}{2} B_0$. The T stress, explained in [16], is due to the eigenvalue $\mu_1 = 1$ when $k = 1$, and the T stress is then: $T = C_1$. The term D_1 due to mode II does not affect the T stress.

The strains in the (r, θ) coordinate system are obtained from substituting the stress components (Appendix A) for the first three eigenvalues $\lambda_n^* = \frac{1}{2}, 1, \frac{3}{2}$ using Hooke's law. Plane stress can be assumed since the strain gauges are mounted on stress free surfaces

$$\varepsilon_{rr} = \frac{1}{E} (\sigma_{rr} - \nu \sigma_{\theta\theta}) \quad (1)$$

$$\varepsilon_{\theta\theta} = \frac{1}{E} (\sigma_{\theta\theta} - \nu \sigma_{rr}) \quad (2)$$

$$\varepsilon_{r\theta} = \frac{1}{2\mu} \sigma_{r\theta} \quad (3)$$

The measured $\alpha\alpha$ strain component is given by:

$$\varepsilon_{\alpha\alpha} = \varepsilon_{rr} \cos^2(\theta - \alpha) + \varepsilon_{\theta\theta} \sin^2(\theta - \alpha) - 2 \cos(\theta - \alpha) \sin(\theta - \alpha) \varepsilon_{r\theta} \quad (4)$$

which can be written as

$$\varepsilon_{\alpha\alpha} = a_0 A_0 + b_0 B_0 + a_1 A_1 + b_1 B_1 + c_1 C_1 \quad (5)$$

where $d_i = [a_0, b_0, a_1, b_1, c_1]^T = f_i(E, \nu, r, \theta, \alpha)$, $i = 1 \dots 5$.

$$a_0 = \frac{1}{8E\sqrt{r}} \left[4(1 - \nu) \cos \frac{\theta}{2} - (1 + \nu) \cos \left(\frac{\theta}{2} - 2\alpha \right) + (1 + \nu) \cos \left(\frac{5\theta}{2} - 2\alpha \right) \right] \quad (6)$$

$$b_0 = \frac{1}{8E\sqrt{r}} \left[-4(1 - \nu) \sin \frac{\theta}{2} - 3(1 + \nu) \sin \left(\frac{\theta}{2} - 2\alpha \right) - (1 + \nu) \sin \left(\frac{5\theta}{2} - 2\alpha \right) \right] \quad (7)$$

$$a_1 = \frac{\sqrt{r}}{8E} \left[4(1 - \nu) \cos \frac{\theta}{2} + (1 + \nu) \cos \left(\frac{\theta}{2} + 2\alpha \right) - (1 + \nu) \cos \left(\frac{3\theta}{2} - 2\alpha \right) \right] \quad (8)$$

$$b_1 = \frac{\sqrt{r}}{8E} \left[4(1 - \nu) \sin \frac{\theta}{2} + 5(1 + \nu) \sin \left(\frac{\theta}{2} + 2\alpha \right) + (1 + \nu) \sin \left(\frac{3\theta}{2} - 2\alpha \right) \right] \quad (9)$$

$$c_1 = \frac{1}{2E} [(1 + \nu) \cos(2\alpha) + 1 - \nu] \quad (10)$$

The choice of an optimal location is discussed next.

3. Optimum location and orientation of a strain gauge

3.1. The single strain gauge

Three parameters must be chosen in mounting a single strain gauge near a crack tip, namely the location in relation to the crack tip (r, θ) , and the orientation angle α . From Eq. (5), only one parameter can be calculated with a single strain gauge,

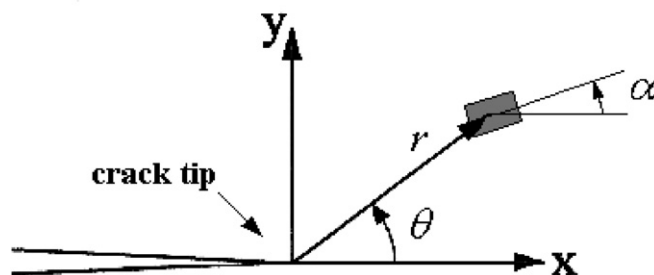


Fig. 1. A strain gauge located at (r, θ) and oriented at an angle α .

namely A_0 for mode I or B_0 for mode II. The coefficients corresponding to $\lambda^* > \frac{1}{2}$ are the truncation errors. In order to be in the K dominant region, where the contribution of the higher order terms of the asymptotic solution are negligible in comparison with the first one, the strain gauges should be placed as close as possible to the crack tip. This means that r should be as small as possible but outside the plastic zone (or) where 3D effects might be strong. Usually the distance r is dictated by the physical size of the strain gauge.

The orientation angle α is usually chosen such as to minimize the effect of the T stress. It can be observed in Eq. (10) that c_1 only depends on ν and α and not on r and θ . With a proper choice of α the coefficient c_1 becomes zero and the effect of the T stress on the strain gauges readings of a strain gauge oriented at α_0 is therefore eliminated.

$$\pm \alpha_0 = \frac{1}{2} \cos^{-1} \left(-\frac{1-\nu}{1+\nu} \right) \quad (11)$$

Eq. (11) was obtained in [7] for a pure mode II displacement field. In [1,2,5,6] for pure mode I. The span of α for all possible ν is: $90^\circ \geq \alpha \geq 54.7^\circ$. In particular, for $\nu = 0.3$, an orientation angle of $\alpha_0 = 61.3^\circ$ will eliminate the effect of the T stress.

The location angle θ is chosen so that the coefficients corresponding to the singular terms $1/\sqrt{r}$, are as large as possible, and the coefficients corresponding to the \sqrt{r} term are minimized. In a mode II field, $A_0 = A_1 = 0$ and the main error in using (5) is due to the term $b_1 B_1$. B_1 depends on the load and boundary conditions and cannot be controlled. An angle minimizing b_1 is desired while b_0 remains large. By analogy, for a mode I field, $B_0 = B_1 = 0$ and the main error in using (5) is due to the term $a_1 A_1$. A_1 depends on the load and boundary conditions and cannot be controlled. An angle minimizing a_1 is desired while keeping a_0 large. The angular distributions of the coefficients A_0 , B_0 and A_1 , B_1 , which correspond to $\lambda = 1/2$ and $\lambda = 3/2$ at orientation angle $\alpha = 61.3^\circ$ are plotted in Fig. 2. The normalized variations of a_0 and a_1 which correspond to A_0 and A_1 (mode I), respectively, are plotted in Fig. 2a while the normalized variation of b_0 and b_1 which correspond to the coefficients B_0 and B_1 (mode II), respectively, are plotted in Fig. 2b. An angle $\theta = 16^\circ$ was chosen by Burgel et al. [7] for mode II calculations. These researchers remarked that since the influence of higher order terms is not eliminated a few strain gauges should be used and an extrapolation should be conducted for obtaining accurate SIF from the strain gauges measurements. Accurate calculation of stress intensity factor of even a single mode requires more than one strain gauge. Since the available space around a crack tip is limited, the use of a rosette appears to be recommended, as discussed next.

3.2. The three strain gauge rosette

A rosette made of three strain gauges is shown in Fig. 3. The rosette is located at a point (r, θ) . Each pair of strain gauges makes an angle β . One of the three strain gauges of the rosette ((1) in Fig. 3) is oriented at an angle α . The measured strains ($\varepsilon_1, \varepsilon_2, \varepsilon_3$), of the rosette can be fitted using Eq. (5) as follows:

$$\begin{Bmatrix} \varepsilon_1(\alpha_1) \\ \varepsilon_2(\alpha_2) \\ \varepsilon_3(\alpha_3) \end{Bmatrix} = \begin{bmatrix} a_0(\alpha_1) & b_0(\alpha_1) & c_1(\alpha_1) \\ a_0(\alpha_2) & b_0(\alpha_2) & c_1(\alpha_2) \\ a_0(\alpha_3) & b_0(\alpha_3) & c_1(\alpha_3) \end{bmatrix} \begin{Bmatrix} A_0 \\ B_0 \\ C_1 \end{Bmatrix} + \begin{Bmatrix} R_1(\alpha_1) \\ R_2(\alpha_2) \\ R_3(\alpha_3) \end{Bmatrix} \quad (12)$$

In (12) $\alpha_1, \alpha_2, \alpha_3$ are the orientation angles of strain gauges of the rosette. The orientation angles α_2, α_3 can be written as: $\alpha_2 = \alpha_1 - \beta$ and $\alpha_3 = \alpha_1 - 2\beta$.

Which can be written in a vector/matrix form

$$\varepsilon = M \cdot A + R \quad (13)$$

where

$$\varepsilon = [\varepsilon_1(\alpha_1) \ \varepsilon_2(\alpha_2) \ \varepsilon_3(\alpha_3)]^T, \quad (13a)$$

$$A = [A_0 \ B_0 \ C_1]^T, \quad (13b)$$

$$R = [R_1(\alpha_1) \ R_2(\alpha_2) \ R_3(\alpha_3)]^T, \quad (13c)$$

and

$$M = \begin{bmatrix} a_0(\alpha_1) & b_0(\alpha_1) & c_1(\alpha_1) \\ a_0(\alpha_2) & b_0(\alpha_2) & c_1(\alpha_2) \\ a_0(\alpha_3) & b_0(\alpha_3) & c_1(\alpha_3) \end{bmatrix} \quad (13d)$$

The coefficients are calculated by

$$A = M^{-1} \varepsilon \quad (14)$$

But from Eq. (12) which does not neglect the truncation error R it should be:

$$A = M^{-1} \varepsilon - M^{-1} R \quad (15)$$

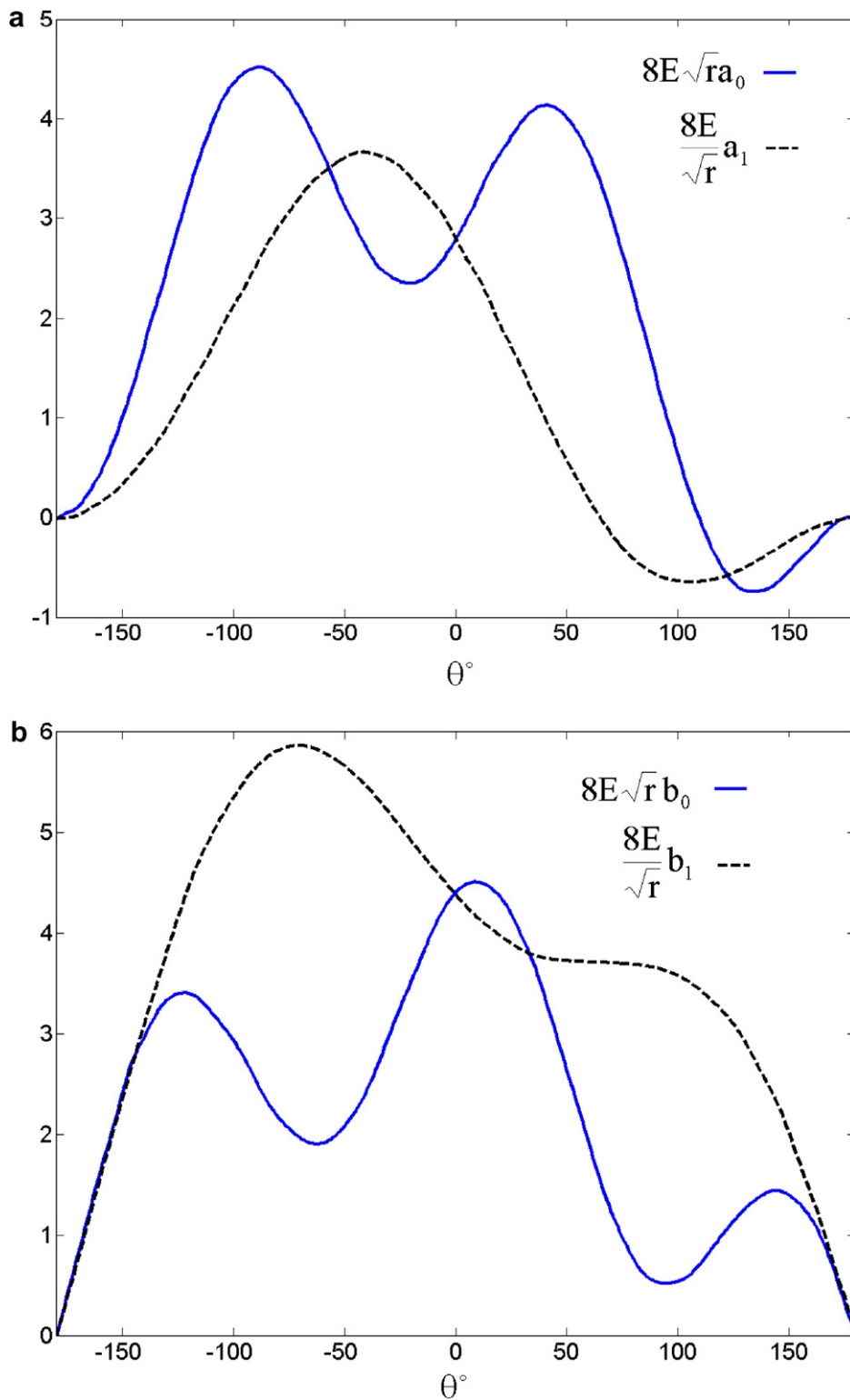


Fig. 2. Angular normal distribution of a_0 , a_1 , b_0 and b_1 for $\alpha = 61.3^\circ$ and $\nu = 0.3$. (a) The normalized variations of a_0 and a_1 which correspond to A_0 and A_1 (mode I), respectively. (b) The normalized variation of b_0 and b_1 which correspond to the coefficients B_0 and B_1 (mode II), respectively.

Therefore the error involved in the calculation of A by Eq. (14) is

$$E_r = -M^{-1}R \quad (16)$$

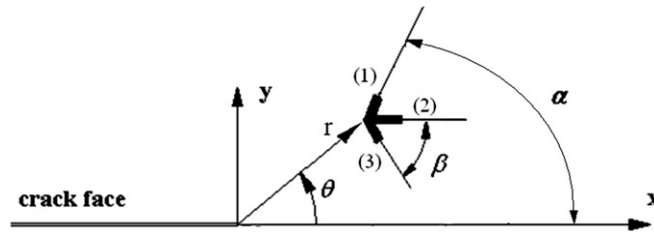


Fig. 3. A rosette made of three gauges ((1), (2) and (3)) with an angle β between them, located at (r, θ) . Gauge (1) is oriented at angle α .

When using three strain gauges for calculating K_I , K_{II} and T , the truncation error is due to the eigenvalues $\lambda_n^* = \frac{n}{2}$, $n \geq 3$. Assuming that the greatest contribution to the truncation error is due to the next largest eigenvalue, $\lambda_n = \frac{3}{2}$, the truncation error can then be estimated by:

$$R = \begin{Bmatrix} R_1(\alpha) \\ R_2(\alpha_2) \\ R_3(\alpha_3) \end{Bmatrix} \cong \begin{Bmatrix} a_1(\alpha_1)A_1 + b_1(\alpha_1)B_1 \\ a_1(\alpha_2)A_1 + b_1(\alpha_2)B_1 \\ a_1(\alpha_3)A_1 + b_1(\alpha_3)B_1 \end{Bmatrix} = A_1 \begin{Bmatrix} a_1(\alpha_1) + \frac{B_1}{A_1}b_1(\alpha_1) \\ a_1(\alpha_2) + \frac{B_1}{A_1}b_1(\alpha_2) \\ a_1(\alpha_3) + \frac{B_1}{A_1}b_1(\alpha_3) \end{Bmatrix} \equiv A_1 \hat{R} \quad (17)$$

The error can be estimated by

$$E_r = -M^{-1}A_1\hat{R} \quad (18)$$

Using Eqs. (5)–(9) and substituting into (12) and performing (16) results in an explicit vector expression for the errors.

$$E_r = \begin{Bmatrix} rA_1 \left(-\cos(\theta) + \frac{B_1}{A_1}(-1 + 3\cos(\theta))\tan\left(\frac{\theta}{2}\right) \right) \\ rA_1 \left(\sin(\theta) + \frac{B_1}{A_1}(-4 + 3\cos(\theta)) \right) \\ -4rA_1 \frac{B_1}{A_1} \frac{1}{\sqrt{r}} \sin\left(\frac{\theta}{2}\right) \end{Bmatrix} \quad (19)$$

Eq. (19) is explicited in Appendix B and does not depend on the orientation angle α_1 which means that the orientation angle α of the rosette does not affect the magnitude of the error related to $\lambda_n = \frac{3}{2}$. Similarly, the parameters β , ν and E do not affect the error as well. The error E_r is found to depend on the location (r, θ) and ν and the magnitude of A_1 and B_1 . The coefficients A_i , B_i , C_i , D_i $i = 1 \dots \infty$, of the asymptotic expansion are dictated by the geometry and the boundary conditions and can not therefore be controlled. It is desired to find a location (r, θ) which will minimize the contribution of A_1 and B_1 to the error (18). As shown in the Appendix B, Eq. (18) is linear with r , and can be put in the form $E_r = rE_r^{(0)}$, meaning that the closer the rosette is to the crack tip, the smaller the error. The optimal orientation angle θ is discussed next. Posing:

$$\frac{B_1}{A_1} = \tan \psi \quad (20)$$

Then $0 \leq \psi \leq 90$ where $\psi = 0^\circ$ correspond to $B_1 = 0$ (pure mode I) and $\psi = 90^\circ$ correspond to $A_1 = 0$ (pure mode II). The error $E_r^{(0)}$ can be normalized by:

$$\hat{E}_r^{(0)}\left(\theta, \frac{B_1}{A_1}\right) = \frac{E_r^{(0)}}{\sqrt{A_1^2 + B_1^2}} = \frac{\frac{E_r}{r}}{\sqrt{A_1^2 + B_1^2}} = -\frac{M^{-1}A_1\hat{R}}{r\sqrt{A_1^2 + B_1^2}} = -\frac{1}{r} \frac{M^{-1}\hat{R}}{\sqrt{1 + \tan^2 \psi}} \quad (21)$$

The error (21) in calculating K_I and K_{II} is plotted in Fig. 4 for seven values of $\frac{B_1}{A_1} = 0.1, 0.2, 0.5, 1.0, 2.0, 5.0$ and 10.0 as a function of θ , corresponding to the angle: $\psi = 5.7^\circ, 11.3^\circ, 26.6^\circ, 45^\circ, 63.4^\circ, 78.7^\circ$ and 84.3° . The calculations use, $\nu = 0.3$. Fig. 4a shows the normalized error in K_I while Fig. 4b shows the normalized error in K_{II} . The normalized errors of K_I and K_{II} as a function of θ in pure mode I ($B_1 = 0, \psi = 0^\circ$) and pure mode II ($A_1 = 0, \psi = 90^\circ$) are plotted in Fig. 5. It can be observed in Fig. 5 that for pure mode I ($\psi = 0^\circ$), the error in K_I (due to $\lambda = 3/2$) can be completely eliminated by choosing $\theta = \pm 90^\circ$. For other values of ψ , a good choice might be $\theta = \pm 75^\circ$. It can also be observed in Fig. 5 that for pure mode II ($\psi = 90^\circ$), the error in K_{II} (due to $\lambda = 3/2$) cannot be completely eliminated, but choosing $\theta = 0^\circ$ will minimize it. The minimum error of K_{II} is the maximum error for K_I . For other values of ψ a good choice for minimizing the error of K_{II} is $0^\circ \leq \theta \leq 20^\circ$. Since the errors in K_{II} are larger than the errors of K_I , $\theta = 0^\circ$ is a good choice when ψ , the mode-mix, is not known *a priori*.

3.3. A numerical example

The problem of an inclined edge crack in a finite plate subjected to tension as seen in Fig. 6a was solved numerically using commercial finite elements code Ansys [17]. In the numerical analysis $a/b = 0.5$ and $b = 40$ mm. The inclination angle was chosen to be $\theta = 45^\circ$. The Young's modulus of the material was $E = 210$ GPa and Poisson's ratio $\nu = 0.3$. The plate was loaded numerically by $\sigma_0 = 200$ MPa. The stress intensity factor solution is given in [18] $\frac{K_I}{K_0} = 1.2$ and $\frac{K_{II}}{K_0} = 0.57$ where $K_0 = \sigma_0\sqrt{\pi a}$.

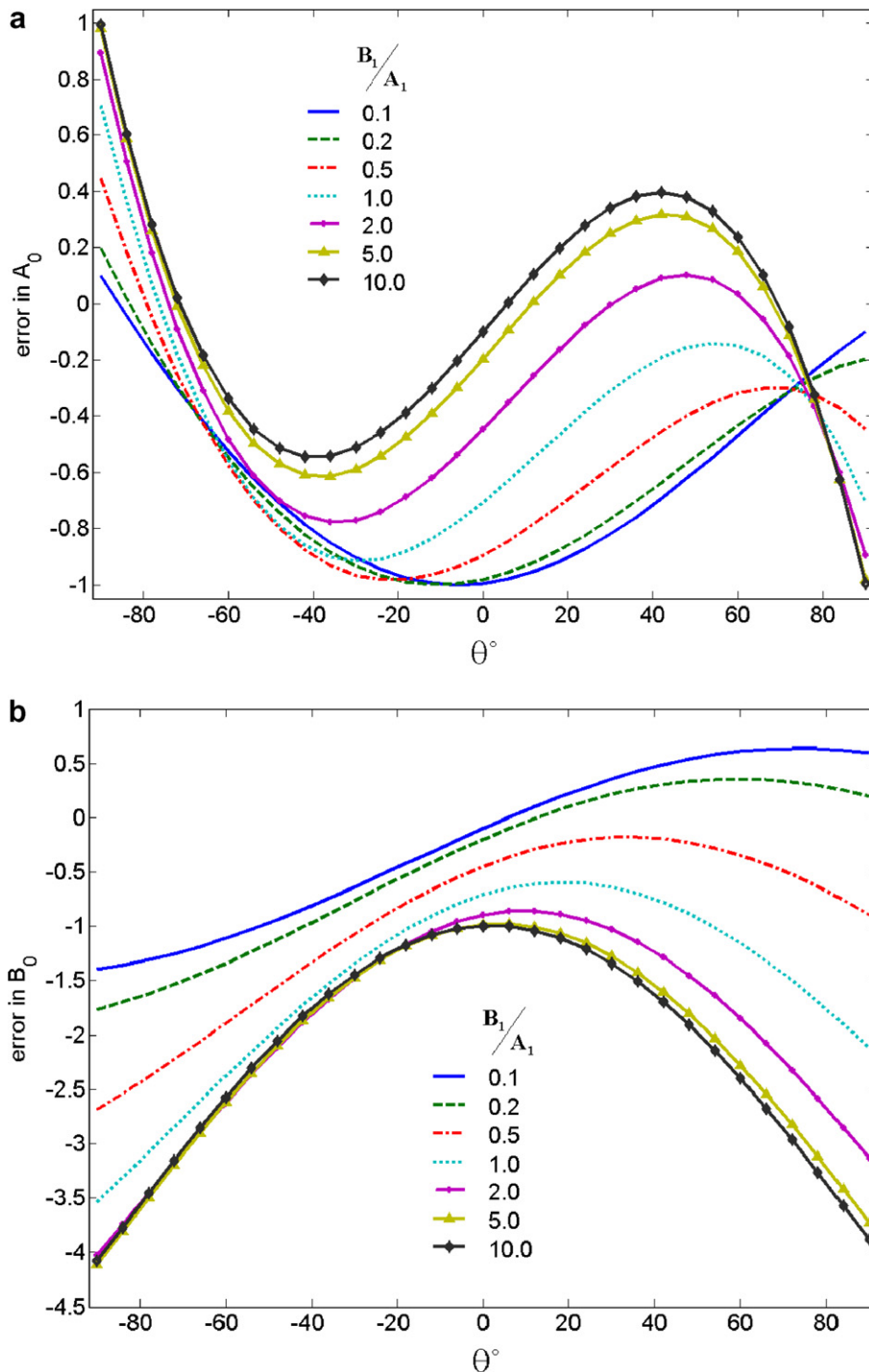


Fig. 4. The errors as a function of θ for $B_1/A_1 = 0.1, 0.2, 0.5, 1.0, 2.0, 5.0$ and 10.0 . (a) For A_0 . (b) For B_0 .

The plate was meshed with 7601 PLANE82 elements with mesh size of 0.2 mm in the vicinity of the crack tip. Plane stress conditions were used. The deformed meshed plate is seen in Fig. 6b. The stress intensity factors were calculated from the crack face displacement and yielded $K_I/K_0 = 1.21$ and $K_{II}/K_0 = -0.56$. These values have less than 1.2% discrepancy from the values given in [18]. It is assumed that a rosette with $\beta = 45^\circ$ between its strain gauges is mounted in front of the crack tip at $\theta = 0$. The calculated strain at the location of the assumed rosette served as “experimental” readings. The stress intensity factors were calculated using (14) and the difference from the values of [18] are plotted as a function of r in Fig. 7.

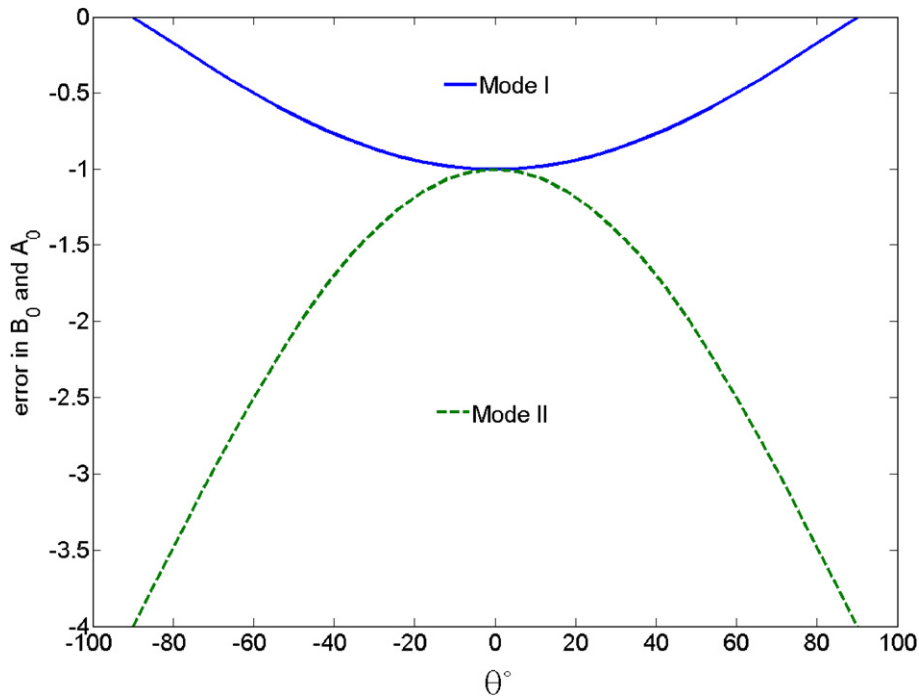


Fig. 5. The normalized errors of K_I and K_{II} as a function of θ in pure mode I ($B_I = 0$, $\psi = 0^\circ$) and pure mode II ($A_I = 0$, $\psi = 90^\circ$).

The error distribution is close to linear with r . The slight departure from an absolutely linear behavior is probably due to numerical inaccuracy close to the crack tip and the presence of higher order terms far from the crack tip. The error is quite large: even at a small distance of $r/a = 0.1$, which is 2 mm from the crack tip, the error in K_I exceeds 20% and more than 10% error for K_{II} . Because of the linear behavior of the error with r , it is recommended to use two rosettes at different radiuses, and linearly extrapolate their results. An error of less than 15% is expected this way. Such an extrapolation is seen in Fig. 7 for the distances $r/a = 0.2$ and $r/a = 0.4$.

4. Discussion

With a single strain gauge, one can only determine one coefficient of the asymptotic expansion which corresponds to the singular term with eigenvalue $\lambda^* = 1/2$. The truncation error for fitting the strain corresponds to $\lambda^* \geq 1$. By proper orientation of the single strain gauge (Eq. (11)) the effect of the T stress ($\lambda^* = 1$) can be eliminated. This elimination enhances the accuracy of the K_I or K_{II} calculated by a single strain gauge in a single mode loading (mode I or mode II correspondingly), since the truncation error in fitting the strain is due to $\lambda^* \geq 3/2$, the next eigenvalue in the asymptotic expansion. Although pure mode II loading does not contribute to the T stress because only the coefficient C_1 does (D_1 of mode II does not), a pure mode II loading is hard to achieve experimentally, and the gauge needs to be oriented according to Eq. (11). A proper location, at which this error is small, leading to accurate SIF calculation has been worked out by many researchers.

However, for dynamic loading configurations, single mode loading may be difficult to achieve, and this might impair the accuracy of SIF determination from a single strain gauge. Another typical problem is that of interfacial cracks where the two modes of loading are coupled. For such cases the minimum number of strain gauges that should be used is two. These two gauges might be oriented to eliminate the effect of the T stress, but the proper locations that will minimize the errors due to $\lambda = 3/2$ and its corresponding two coefficients A_1 and B_1 must be determined according their ratio. An alternative to two separate strain gauges is a two-gauge rosette that measures the strains at the same nominal point, which, in addition to static experiments, is particularly advantageous in dynamic loading situations, where different stresses are experienced at different times. Hence the use of the double strain gauge rosette is preferred, but the two strain gauges cannot be oriented to the same direction in order to eliminate the T stress. Consequently a third strain gauge is needed, if only errors due to $\lambda^* \geq 3/2$ are desired.

A rosette comprising three strain gauges all located at one same point, is capable of determining the first three coefficients of the asymptotic expansion with errors only due to $\lambda^* \geq 3/2$. This investigation has characterized the errors in calculating K_I and/or K_{II} in a mixed mode loading. A numerical example has been brought to illustrate the above mentioned point. An interesting outcome of this study is that the error in the estimation of the SIFs is linear in r and does not depend on the orientation angle α . It is also independent of the material properties and the angle between the individual strain gages in the rosette. However, the overall error is still non-negligible when a single rosette is cemented at practical distances from the crack tip. Therefore, one way to reduce the error is to use two rosettes and perform an extrapolation of the SIF to very small rs .

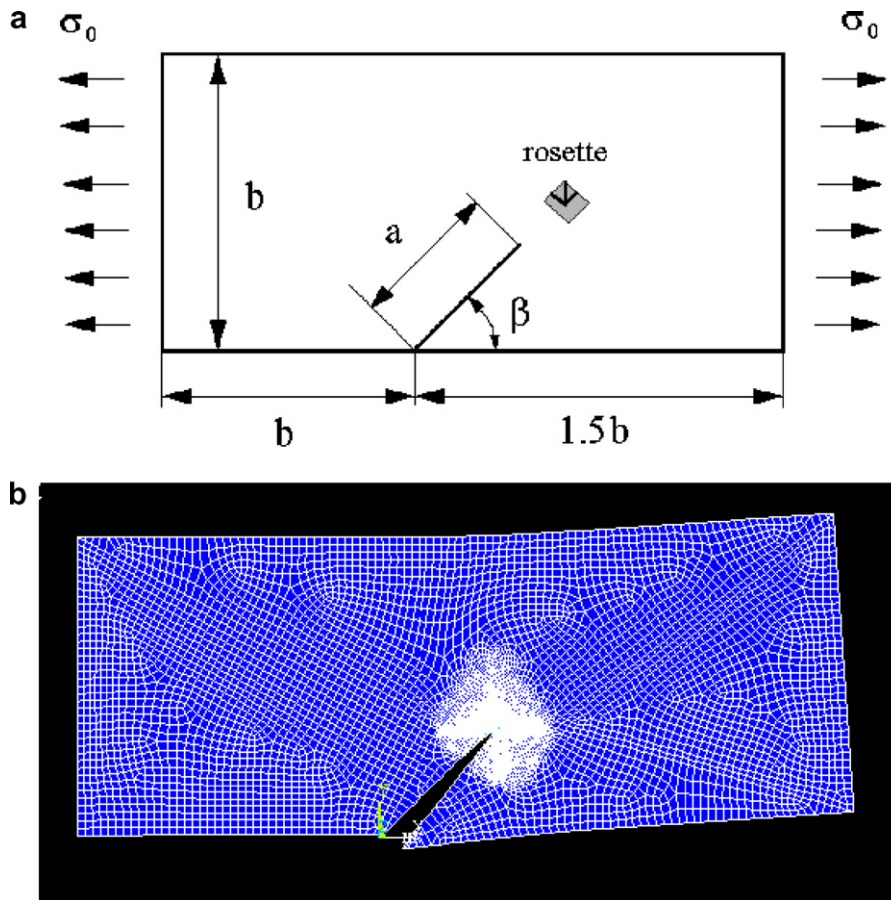


Fig. 6. (a) A finite plate with an inclined edge crack loaded in tension. (b) The deformed meshed plate.

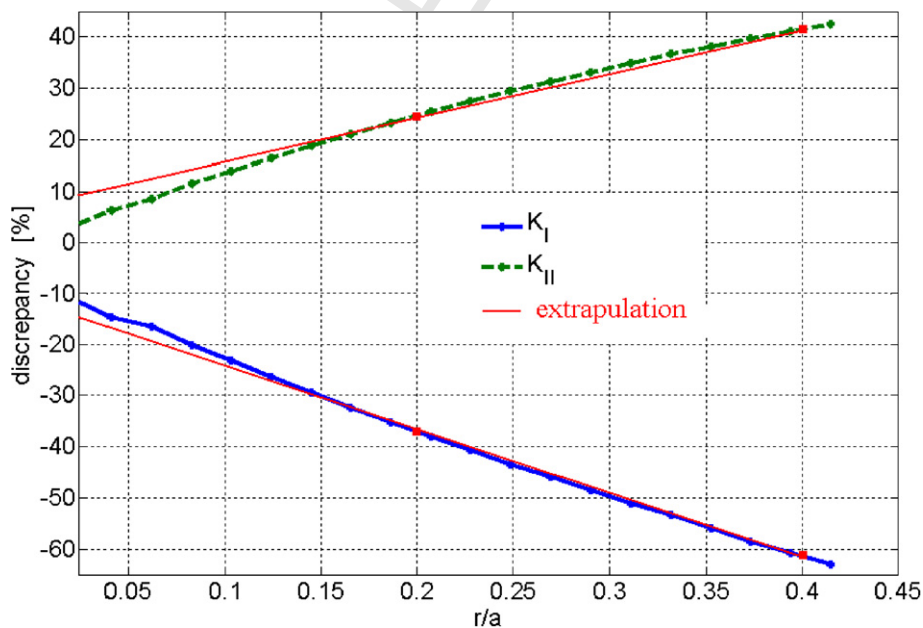


Fig. 7. Errors in K_I and K_{II} vs. the distance from crack tip.

These guidelines are expected to assist the practitioner in the selection of an appropriate combination of strain gauges for a specific problem, together with *a priori* assessment of the error involved in the adopted process.

5. Summary and conclusions

The errors in calculating stress intensity factors from data obtained from a three strain gauge rosette have been investigated. It has been pointed out that the errors are mainly due the eigenvalue $\lambda = 3/2$ and the coefficients A_1 and B_1 which correspond to this eigenvalue. The variation of the normalized errors with θ at any r due to different ratios of A_1 and B_1 have been computed and the following conclusions have been derived:

- The main error in fitting the strain is due to $\lambda = 3/2$, with a linear dependence on \sqrt{r} .
- The errors in the SIF are linear in r .
- Minimizing r will decrease the errors due to higher order terms of the asymptotic expansion.
- The errors are independent of the orientation angle α , the material properties and the angle between the individual elements in the rosette.
- The errors depend only on the location (r, θ) and the coefficients A_1 and B_1 .
- For pure mode I $\theta = \pm 90^\circ$ will completely eliminate the error due to $\lambda = 3/2$.
- For pure mode II $\theta = 0^\circ$ will minimize the error due to $\lambda = 3/2$.
- The maximum error for mode I is at $\theta = 0$, which is the minimum error for mode II at the same angle.
- The proper choice of θ depends on the desired error, namely in K_I , K_{II} or any combination between them.
- It is recommended to use two rosettes at the same θ , and linearly extrapolate their results if errors less than $\sim 15\%$ in a mixed mode field are desired.
- Closer points to the crack tip might even yield an improved accuracy, but three-dimensional effects should be avoided.

Appendix A. Asymptotic solution for a crack in mixed mode loading

The asymptotic solution for the stresses near a crack tip is due to the eigenvalues $\lambda^* = \frac{n}{2}, n = 1 \dots \infty$. To properly impose the free crack face boundary conditions these eigenvalues are split into two sets: $\lambda_n = n + \frac{1}{2}, n = 0 \dots \infty$ and $\mu_k = k, k = 1 \dots \infty$. The solution due to the eigenvalues $\lambda_n = n + \frac{1}{2}, n = 0 \dots \infty$ is

$$\sigma_{rr} = \sum_{n=0}^{\infty} \left\{ -\frac{1}{4} A_n r^{n-\frac{1}{2}} \left[\left(n - \frac{5}{2} \right) \cos \left(n - \frac{1}{2} \right) \theta - \left(n - \frac{1}{2} \right) \cos \left(n + \frac{3}{2} \right) \theta \right] - \frac{1}{4} B_n r^{n-\frac{1}{2}} \left[\left(n - \frac{5}{2} \right) \sin \left(n - \frac{1}{2} \right) \theta - \left(n + \frac{3}{2} \right) \sin \left(n + \frac{3}{2} \right) \theta \right] \right\} \quad (A.1)$$

$$\sigma_{\theta\theta} = \sum_{n=0}^{\infty} \left\{ \frac{1}{4} A_n r^{n-\frac{1}{2}} \left[\left(n + \frac{3}{2} \right) \cos \left(n - \frac{1}{2} \right) \theta - \left(n - \frac{1}{2} \right) \cos \left(n + \frac{3}{2} \right) \theta \right] + \frac{1}{4} B_n r^{n-\frac{1}{2}} \left[\left(n + \frac{3}{2} \right) \sin \left(n - \frac{1}{2} \right) \theta - \left(n + \frac{3}{2} \right) \sin \left(n + \frac{3}{2} \right) \theta \right] \right\} \quad (A.2)$$

$$\sigma_{r\theta} = \sum_{n=0}^{\infty} \left\{ \frac{1}{4} A_n r^{n-\frac{1}{2}} \left(n - \frac{1}{2} \right) \left[\sin \left(n - \frac{1}{2} \right) \theta - \sin \left(n + \frac{3}{2} \right) \theta \right] - \frac{1}{4} B_n r^{n-\frac{1}{2}} \left[\left(n - \frac{1}{2} \right) \cos \left(n - \frac{1}{2} \right) \theta - \left(n + \frac{3}{2} \right) \cos \left(n + \frac{3}{2} \right) \theta \right] \right\} \quad (A.3)$$

The singular solution is due to $n = 0$ and hence $\lambda_0 = \frac{1}{2}$. The conventional stress intensity factors are related to the constants A_0 and B_0 by:

$$K_I = \frac{\sqrt{2\pi}}{2} A_0 \quad (A.4)$$

$$K_{II} = \frac{\sqrt{2\pi}}{2} B_0 \quad (A.5)$$

The asymptotic solution for the stresses near a crack tip due to the eigen value $\mu_k = k, k = 1 \dots \infty$.

$$\sigma_{rr} = \sum_{k=1}^{\infty} \left\{ \frac{1}{2} C_k r^{k-1} [2 \cos(k\theta) \cos(\theta) + (1-k) \sin(k\theta) \sin(\theta)] + \frac{1}{2} D_k r^{k-1} [\sin(k\theta) \cos(\theta) - (2-k) \cos(k\theta) \sin(\theta)] \right\} \quad (A.6)$$

$$\sigma_{\theta\theta} = \sum_{k=1}^{\infty} \left\{ \frac{1}{2} C_k r^{k-1} (1+k) \sin(k\theta) \sin(\theta) + \frac{1}{2} D_k r^{k-1} [\sin(k\theta) \cos(\theta) - k \cos(k\theta) \sin(\theta)] \right\} \quad (A.7)$$

$$\sigma_{r\theta} = \sum_{k=1}^{\infty} \left\{ -\frac{1}{2} C_k r^{k-1} [\sin(k\theta) \cos(\theta) + k \cos(k\theta) \sin(\theta)] + \frac{1}{2} D_k r^{k-1} (1-k) \sin(k\theta) \sin(\theta) \right\} \quad (A.8)$$

Appendix B. Parametric error calculation

```

% A MATLAB program for calculating analytically the errors
% involved in calculating stress intensity factors from
% the strain measurements of a strain gauge rosette.
clear all
close all
%
syms a1 b1 c1 d1 e1 a2 b2 c2 d2 e2 a3 b3 c3 d3 e3 A B eps1 eps2 eps3
syms E nu r theta alpha alpha1 alpha2 alpha3 beta
%
con1 = 1/(8 * E * sqrt(r));
con2 = 1/(2 * E);
con3 = sqrt(r)/(8 * E);
%
t1 = theta/2;
t2m = t1 - 2 * alpha;
t2p = t1 + 2 * alpha;
t3m = 3 * t1 - 2 * alpha;
t5m = 5 * t1 - 2 * alpha;
%
ct1 = cos(t1);
st1 = sin(t1);
st2m = sin(t2m);
ct2m = cos(t2m);
st2p = sin(t2p);
ct2p = cos(t2p);
st3m = sin(t3m);
ct3m = cos(t3m);
st5m = sin(t5m);
ct5m = cos(t5m);
% p1 is Eq. (6)
p1 = con1 * (4 * (1-nu) * ct1 - (1+nu) * ct2m + (1+nu) * ct5m);
% p2 is Eq. (7)
p2 = con1 * (-4 * (1-nu) * st1 - 3 * (1+nu) * st2m - (1+nu) * st5m);
% p3 is Eq. (10)
p3 = con2 * ((1+nu) * cos(2 * alpha) + 1 - nu);
% q1 is Eq. (8)
q1 = con3 * (4 * (1-nu) * ct1 + (1+nu) * ct2p - (1+nu) * ct3m);
% q2 is Eq. (9)
q2 = con3 * (4 * (1-nu) * st1 + 5 * (1+nu) * st2p + (1+nu) * st3m);
%creating the components of Eq. (13)
a11 = subs(p1,alpha,alpha1);
b11 = subs(p2,alpha,alpha1);
c11 = subs(p3,alpha,alpha1);
d11 = subs(q1,alpha,alpha1);
e11 = subs(q2,alpha,alpha1);

a22 = subs(p1,alpha,alpha2);
b22 = subs(p2,alpha,alpha2);
c22 = subs(p3,alpha,alpha2);
d22 = subs(q1,alpha,alpha2);
e22 = subs(q2,alpha,alpha2);

a33 = subs(p1,alpha,alpha3);
b33 = subs(p2,alpha,alpha3);
c33 = subs(p3,alpha,alpha3);
d33 = subs(q1,alpha,alpha3);

```

```

329     e33 = subs(q2,alpha,alpha3);
330
331     % the truncation errors
332     R1 = d1*A + e1*B;
333     R2 = d2*A + e2*B;
334     R3 = d3*A + e3*B;
335
336     v = [eps1 - R1; eps2 - R2; eps3 - R3];
337     v1 = [eps1; eps2; eps3];
338     % calculating Eq. (16)
339     M = [a1 b1 c1; a2 b2 c2; a3 b3 c3];
340     solu = inv(M) * (v - v1);
341
342     resid1 = collect(simple(solu(1)),B);
343     resid1 = collect(resid1,A);
344
345     resid2 = collect(simple(solu(2)),B);
346     resid2 = collect(resid2,A);
347
348     resid3 = collect(simple(solu(3)),B);
349     resid3 = collect(resid3,A);
350
351     % substituting the components
352     % R11 is the error in KI
353     % R22 is the error in KII
354     % R33 is the error of T
355
356     R1 = subs(resid1,{a1,b1,c1,d1,e1,a2,b2,c2,d2,e2,a3,b3,c3,d3,e3},{a11,b11,
357     c11,d11,e11,a22,b22,c22,d22,e22,a33,b33,c33,d33,e33});
358     R11 = subs(R1,{alpha2,alpha3},{alpha1-beta,alpha1-2 beta});
359     R11 = collect(R11,E);
360     dR11_1 = diff(R11,E);
361     dR11_2 = diff(R11,alpha1);
362     dR11_2 = expand(dR11_2);
363     dR11_3 = diff(R11,beta);
364     %%%%%%%%%%%%%%%%%%%%%%%%%%%%%%%%%%%%%%%%%%%%%%%%%%%%%%%%%%%%%%%%%%%%%%%%%
365     R2 = subs(resid2,{a1,b1,c1,d1,e1,a2,b2,c2,d2,e2,a3,b3,c3,d3,e3},{a11,b11,
366     c11,d11,e11,a22,b22,c22,d22,e22,a33,b33,c33,d33,e33});
367     R22 = subs(R2,{alpha2,alpha3},{alpha1-beta,alpha1-2 beta});
368     R22 = collect(R22,E);
369     dR22_1 = diff(R22,E);
370     dR22_2 = diff(R22,alpha1);
371     dR22_2 = expand(dR22_2);
372     dR22_3 = diff(R22,beta);
373     %%%%%%%%%%%%%%%%%%%%%%%%%%%%%%%%%%%%%%%%%%%%%%%%%%%%%%%%%%%%%%%%%%%%%%%%%
374     R3 = subs(resid3,{a1,b1,c1,d1,e1,a2,b2,c2,d2,e2,a3,b3,c3,d3,e3},{a11,b11,
375     c11,d11,e11,a22,b22,c22,d22,e22,a33,b33,c33,d33,e33});
376     R33 = subs(R3,{alpha2,alpha3},{alpha1-beta,alpha1-2 beta});
377     R33 = collect(R33,E);
378     dR33_1 = diff(R33,E);
379     dR33_2 = diff(R33,alpha1);
380     dR33_2 = expand(dR33_2);
381     dR33_3 = diff(R33,beta);
382     %%%%%%%%%%%%%%%%%%%%%%%%%%%%%%%%%%%%%%%%%%%%%%%%%%%%%%%%%%%%%%%%%%%%%%%%%
383     % These are the errors of Eq. (18) for AO and BO
384     pretty(R11)
385     pretty(R22)

```

References

- [1] Shukla A. Dynamic fracture mechanics. World Scientific; 2006.
- [2] Dally JW, Sanford RJ. Strain-gage methods for measuring the opening-mode stress-intensity factor K_I . Exp Mech 1987;27:381–8.
- [3] Dally JW, Sanford RJ. Measuring the stress intensity factor for propagating cracks with strain gages. J Test Eval 1990;18:240–9.
- [4] Shukla A, Agrawal BD, Bhushan B. Determination of stress intensity factor in orthotropic composite materials using strain gages. Engng Fract Mech 1989;32:469–77.
- [5] Kuang JH, Chen LS. A single strain gage method for K_I measurement. Engng Fract Mech 1995;51:871–8.
- [6] Parnas I, Bilir OG, Tezcan E. Strain gage methods for measurement of opening mode stress intensity factor. Engng Fract Mech 1996;55:485–92.
- [7] Burgel A, Shin HS, Bergmanshoff D, Kalthoff JF. Optimization of the strain-gauge-method for measuring mode-II stress intensity factors. In: The VIIIth bilateral Czech/German symposium: significance of hybrid method for assessment of reliability and durability in engineering science, 1999.
- [8] Wei J, Zhao JH. A two-strain-gage technique for determining mode I stress-intensity factor. Theor Appl Fract Mech 1997;28:135–40.
- [9] Kondo T, Kobayashi M, Sekine H. Strain gage method for determining stress intensities of sharp-notched strips. Exp Mech 2001;41:1–7.
- [10] Maleski MJ, Kirugulige MS, Tippur HV. A method for measuring mode I crack tip constraint under static and dynamic loading conditions. Exp Mech 2004;44:522–32.
- [11] Ricci V, Shukla A, Singh RP. Evaluation of fracture mechanics parameters in bimaterial systems using strain gages. Engng Fract Mech 1997;58:273–83.
- [12] Marur PR, Tippur HV. A strain gage method for determination of fracture parameters in bimaterial systems. Engng Fract Mech 1999;64:87–104.
- [13] Marur PR, Tippur HV. Dynamic response of bimaterial and graded interface cracks under impact loading. Int J Fract 2000;103:95–109.
- [14] Irwin GR. Analysis of stresses and strains near the end of a crack transversing a plate. J Appl Mech 1957;24:361–4.
- [15] Williams ML. On the stress distribution at the base of a stationary crack. J Appl Mech 1957;24:109–14.
- [16] Anderson TL. Fracture mechanics fundamentals and applications. 3rd ed. CRC Press; 2005.
- [17] Ansys, Release 9.0, ANSYS Inc.
- [18] Rooke DP, Cartwright DJ. Compendium of stress intensity factors. London: HMSO; 1976.